Development of Air-lifted Artificial Upwelling Powered by Wave

Jiawang Chen
Ocean college
Zhejiang University, Hangzhou 310058,China
arwang@zju.edu.cn

Ying Chen
Ocean college
Zhejiang University, Hangzhou 310058,China
ychen@zju.edu.cn

Jing Yang
State Key Lab of Fluid Power Transmission and Control
Zhejiang University, Hangzhou 310027,China
yangjingtx@163.com

Naikuang Liang
Department of engineering Science and Ocean Engineering
National Taiwan University, Taipei 10617,Taiwan(R.O.C)
liangnk@ntu.edu.tw

Shan Lin
State Key Lab of Fluid Power Transmission and Control
Zhejiang University, Hangzhou 310027,China
linshan0520@zju.edu.cn

Han Ge
Ocean college
Zhejiang University, Hangzhou 310058,China
gehan@zju.edu.cn

Wei Fan
Department of ocean engineering
Hangzhou Dianzi University, Hangzhou 310018,China
weifan@163.com

Haocai Huang
Ocean college
Zhejiang University, Hangzhou 310058,China
hchuang@zju.edu.cn

Abstract—*this paper presents that an artificial upwelling system integrated with air-lift upwelling tube and wave powered air booster. The upwelling flow had proved that the air-water mixture flow upward in upwelling tube immersed water can make the underwater at bottom flow upward too. This paper introduces the wave power to collect and pump air into water in one depth of upwelling tube. Meanwhile in the deep water far from the continent, the nutrition concentration near the seabed is higher than that near the surface of sea. On the contrary, the oxygen concentration near the seabed is less than that on the top. The upwelling flow is an available method to balance or decrease the difference of characters between surface and bottom water in the sea, which can improve the environment of marine ranching, and promote the growth of the bottom of the biological food chain. One project - air-lifted artificial upwelling powered by wave had been applied and carried on. In order to confirm the air-lifted upwelling efficiency, 2 lake experiments were finished in Qiandao Lake, The first experiment was done directly with a plastic hose, while at the second experiment, the upwelling tube made of tensional cloth is supported by steel supporting rings, these experiments showed that the efficiency of upwelling flow of the plastic hose is higher than that of upwelling tube with supporting rings, an upwelling tube shrinkage deformation happens easily in the case of large upwelling flow. In addition, a simulation platform was designed and numerical simulated, which simulate the wave lifting and dropping the buoyant ball then get compressed air, whose aim is to get the performance of air collecting and compressing capacity and the efficiency between the hydraulic power and compressed air power.*

Keywords—Artificial upwelling, air-lifted upwelling, wave powered air booster, numerical simulation of prototype.

I. INTRODUCTION

The ocean provides up to 20% of the world's food supply. However, it has recently estimated that 75% of the world's commercial fish stocks are being fished at or above mean sustainable levels [1-2]. On the other hand, Algae fuel might be an alternative to fossil fuel and uses algae as its source of natural deposits[3]. It is time to find ways to increase the resource by developing techniques which enhance productivity in a sustainable way[2].

Artificial submarine mountains were eventually formed through sinking the caisson made with cement and limestone mixed down to the seafloor, in which field Japan has conducted massive testing work, according to a survey from the Ministry of Agriculture, Forestry & Fisheries in Japan, since 1997 when caisson projects were set in Nagasaki and other places, 'the fish yield has reached six times that of the previous'. This approach also has its disadvantage, i.e. it will conflict with the development of oil gas, mineral and other resources from oceans in the future. Moreover, whether it will pollute the marine environment to throw amounts of construction materials to the seafloor remains to be observed. Additionally, the large-scale marine platform scheme employed in Japan,

This work was supported by the the National Natural Science Foundation of China (No. 51120195001) and the Program for Zhejiang Leading Team of S&T Innovation No.2010R50036.

978-0-933957-40-4 ©2013 MTS

which adopted the water-pumping manner to achieve the improvement of the submarine nutrients, was called the TAKUMI equipment (2003)[4].

Isaacs proposed to extract deep-sea water by the wave pump [2, 5-7] , with the simple principle that under the floater on the surface of water, a long tube was vertically installed with a one-way valve inside, which would shut off when the floater moved vertically upward with the waves, otherwise it would open, when the deep-sea water could unidirectionally reach the surface. The flow rate of the upstream proved associated with the wave height and period, as well as the pump efficiency, etc.. Liu developed an artificial upstream device by wave pump (1995, 1999) [5-6] , consisting of a 4m-diameter floater, a riser with diameter of 1.2m and length of 300m, and a flow control valve, which has always been employed for tests in the waters near Hawaii, with the purpose of researching into the influence of large-scale seawater disturbance on the marine microbiological system.

Two types of upstream devices were designed by the US Atmocean company in 2006, one with the hose and the other tubeless[8], employed the wave pump to drive the piston up and down, and that was how the bottom seawater was eventually raised to the surface; While the latter achieved the seawater elevation relying on the wave energy and the seawater mixing on the tide energy, which would get the elevated seawater and nutrients to evenly spread to the surrounding seawater.

In many tropical and subtropical waters, the salinity and temperature of the surface water are greater than those of the bottom water. When the hotter water layer with higher salinity is above the colder one with lower salinity, the salt finger phenomenon will occur[9] , i.e. part of the water with higher salinity will sink down in finger shape, while that with lower salinity will rise to generate upwelling flow, which requires no energy except for inserting some standpipes in the ocean, provided with the initial piping. Based on this principle, Lovelock and Rapley (2007)[10] proposed a scheme to place thousands of plastic pipes (each 300～600 feet in length and 30 feet in diameter) into the ocean to form the artificial standpipe-type upstream, which, however, could not guarantee the upstream formation over full time and space in the deployed ocean field[11].

It requires very small pumping head but large flow to pump the deep-sea water to the ocean surface to improve the fishery ecological environment, and it is necessary to take the deep-sea water pressure, corrosion and marine arrangement, etc. into consideration, consequently, the general pump with high head and small flow could not satisfy. So as to improve the efficiency of the upwelling, Liang and Peng [12-13] applied the air-lift theory to the artificial upwelling, wherein the compressed air was pumped into the vertical tubes in the ocean, and for the mixture of bubbles and water is lighter than seawater, the seawater will rise driven by the kinetic energy of the floating-up bubbles, thereby the deep-sea water rich in high nutrients were eventually elevated to the top to increase the marine productivity, improve the marine environmental conditions, and provide marine culture and propagation with a feasible approach. Liang and Peng [12] conducted theoretical research on the influences of the geometric parameters of the upwelling by the air-powered pump (with tube) and bubble curtain (tubeless), etc., and the latter was obviously much more efficient than the former, nevertheless, the air-outlet section of the latter was placed below the water layer to be lift, which raised higher demand on the power of the air compressor. While for the former, as long as the air outlet was placed on one section inside the pipe, the deep-sea water could be brought upward. Furthermore, the research suggested that with the increasing tube diameter, the flow ratio of water and air could be significantly increased, and the seawater-lift efficiency of the artificial upwelling by the bubble-curtain type could be tens of times that by the water pump one, which, however, has not yet fully been experimentally verified.

McClimans,etc.(2010) [14] studied the seawater-lift method by the bubble curtain, and a 100m-long bubble curtain was designed with the air outlet located 40m underwater. They conducted artificial upwelling test in the Arna fjord in western Norway, wherein the deep-sea water could be lifted at 65m^3/s with 44Nm^3 air injection, which verified the theory of Liang and Peng (2005)[12] . A few days later, the mixed layer between 5-15m inside the Arna fjord was covered by nutritious seawater. Nevertheless, its requirement of traditional energy consumption has lowered its applicable feasibility. But if the wave-power air-lift device could provide sufficient air pressure and flow, the bubble curtain could be employed to create artificial upwelling.

The starting point of this project was to achieve the exchanging of the deep-sea water and the upper water without external power by utilizing the high efficiency of the air-lift upwelling, wherein the waves existing everywhere in the ocean was employed for gas collection and compression, which would then injected into the upwelling tubes at certain depth.

II. AIR-LIFT ARTIFICIAL UPWELLING

A. *Air-lift upwelling theory*

Fan and Chen[15] extended the power balance equation for artificial upwelling (Liang and Peng, 2005) [12]to include the effects of the gas void fraction and the local head loss. The power balance equation as follows:

$$E_i = E_o + E_k + E_{ru} + E_{rd} + E_l + E_e + E_{rise} + E_s \qquad (1)$$

Where E_e is the entrance frictional loss power, E_f is the total frictional loss, E_i is the air input power, E_k is the kinetic energy of the upwelling water, E_o is the power demand of the density difference head, E_{ru} is the frictional loss power in the upper pipe, E_{rd} is the frictional loss power in the low pipe, E_l is the local head loss, E_{rise} is the power demand of the sea surface rise, E_s is the frictional loss power of the sliding (relative) speed between the bubble and the water.

Then a numerical model of the air-lift artificial upwelling has been presented:

where, Q_a is the volume air flow rate at atmospheric pressure, Q_w is the volume water flow rate, given by $Q_w = (\pi/4)D^2 \upsilon_w$, υ_w is the mean velocity of the water in vertical upflow, D is the diameter of upwelling pipe, h_u is the pipe length above air injection, h_0 is the submerged depth of pipe outlet, h_c is the constant of depth ($h_c = 1\text{m}$), P_e is the pressure at the air tube outlet, P_u is the pressure at the upwelling pipe outlet, P_0 is the atmospheric pressure, ρ_m is the density of air water mixture, ρ_d is the density of water at the upwelling pipe inlet (point C ,see Fig.1), ρ_a is the density of air, ρ_0 is the density of water at the upwelling pipe outlet (point O ,see Fig.1) , while g is the gravitational acceleration.

Equation (2) can address two basic air-lift design problems. First, calculation of the water pumping rate Q_w for a given air flow rate Q_a . Second, calculation of the air flow rate Q_a needed to obtain a prescribed liquid pumping rate Q_w .

$$
\begin{aligned}
& Q_a P_0 \ln\left(1+\frac{\left(Q_w \rho_d \left(0.1(h_0+0.5h_u)+h_c\right)+Q_a \rho_a h_c\right) g h_u}{\left(Q_a h_c + Q_w \left(0.1(h_0+0.5h_u)+h_c\right)\right)(P_0+\rho_0 g h_0)} \right) = \\
& = \left(\frac{\rho_d}{2A^2} + \xi_e \frac{\rho_d}{2A^2} + 0.01227 \cdot \frac{h_d \rho_d}{2DA^2} \right) Q_w{}^3 + \frac{0.7543}{\left(\frac{4}{\pi D v}\right)^{0.38}} \cdot \frac{h_d \rho_d}{2DA^2} Q_w{}^{2.62} \\
& + k \frac{Q_w^2}{2gA^2} + 0.01227 \frac{\rho_d}{2} \upsilon_m \frac{h_u}{D} Q_w + \frac{0.7543}{\left(\frac{4}{\pi D v}\right)^{0.38}} \frac{\rho_d}{2} \upsilon_m \frac{h_u}{D} Q_w{}^{0.62} \\
& + \rho_d g h_r Q_w + Q_w \frac{\rho_d}{\rho_0} g \int_0^{h_u+h_d} \left(\rho(l)-\rho_0\right) dl
\end{aligned}
\qquad (2)
$$

The robust performance of the model has been confirmed by the experimental findings. The results show that the air-lift upwelling model is feasible to predict the performance of the air-lift pump. Computationally, the model is stable and possess accuracy. The presented theoretical model can be utilized during various stages of the design of an air-lift artificial upwelling system to help evaluate the performance of a pump under predetermined operating conditions, and to select optimal process parameters and to address possible problems.

The efficiency of the air-lift artificial upwelling is shown to be strongly dependent on the geometrical parameters of upwelling pipe, type of air injection nozzle and air volume flow rate. Based on the Eq.2, it is found that the upwelling flow lifting efficiency increases with the increase of the pipe diameter due to the reduction of the friction in the upwelling pipe. Experimental results confirm that the air-lift artificial upwelling is an effective method for upwelling deep (see fig.4), nutrient-rich waters into the euphotic zone to feed phytoplankton and mimicking natural upwelling which sustains the most productive ocean fishing grounds in the world.

B. Air-lift upwelling tests

In September 2011 and December 2012, we deployed the air-lift upwelling assembly to the Qiandao Lake (29°33′51" N , 119°11′9" E). Fig.1 shows the schematic diagram of the experimental set-up. A vertical pipe with 28m length and different internal diameters (0.4m, 0.5m, 1.0m, 1.5m, 2.0m) was deployed. It was composed of a water suction pipe ($h_d = 20m$) and a gas injection section pipe ($h_u = 8m$). The pipe was totally submerged vertically in water and the submerged depth of pipe outlet was h_0 ($h_0 = 2.1m$). An air compressor (Model W-0.36/8) was the air supplier of the experiment. Air went from the air compressor through a 15mm diameter tube to an on/off valve, then to a pressure control valve, where the pressure was reduced to the working pressure (1.2-3.2 Bar). The air then went through a mass-flow meter which was used to control the constant air flow rates. Air was metered and the volume flow rate was determined from the reading of upstream pressure and the temperature together with the reading of the mass-flow meter of gas. Compressed air was delivered at point B through an external pipe.

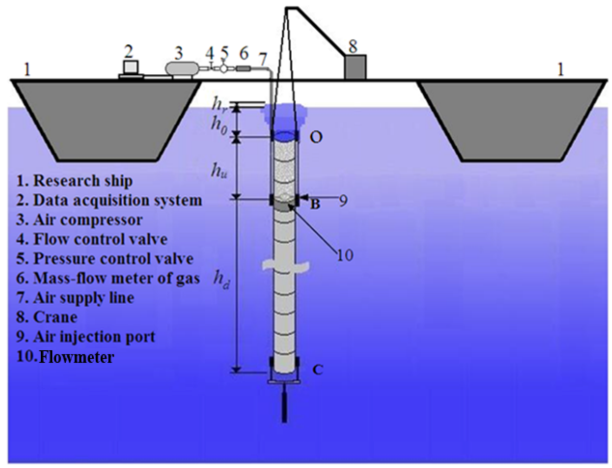

Fig. 1. A schematic diagram of the air-lift pump for artificial upwelling of deep water.

In the suction pipe, between points B and C, there was only water flowing, while all of the gas injection section (between points B and O) was occupied by the two-phase water-air flow. Four different air injection nozzle designs were used with different air flow rates (from 1.9 to 55 m^3/h). The nozzles were made of stainless steel and placed at the center of the upwelling pipe so that the bubbles free themselves easier and do not cling to the pipe wall. At first lake test, an electromagnetic flowmeter, Model MGG/KLL-magB, was installed in vertical upward pipe at the bottom of the gas injection section. And at the second lake test, the ultrasonic flowmeter was replaced the electromagnetic flowmeter due to the fixed dimensions of the flange joint, and the ultrasonic flowmeter could be installed freely. A water level sensor (Model 280-WL400) was used to record the water level dynamics. The pressure losses in the upwelling pipe were obtained by linking six pressure transducers which located throughout the upwelling pipe to the data collection system through a waterproof electrical cable.

According to Eq.(1), the structure-related influencing factor was the shape of the upwelling tube, considering the pipe diameter and the roughness of its inner surface. The lake tests were conducted twice in total, wherein air-lift upwelling test was respectively conducted on upwelling tubes of two structural types, which could be employed to measure the influence of two different structures on the upwelling efficiency.

Fig. 2. Structures of the upwelling tubes: (a) the ventilation pipe directly applied; (b) the upwelling tube with inner support rings

The first upwelling tube was a inner corrugation-shaped ventilation one (see fig.2(a)), which could be directly purchased from the market, whose diameter, however, is monotonic with dimensions rather limited, and those with diameter larger than 1m need to be customized; moreover, the tube structure was so fixed, the larger the diameter, the more difficult the transportation and installation. The second upwelling tube employed the nylon sleeve structure with inner support rings and outer flexible nylon tube, which imitated the first structure, and its greatest advantage over the former lied in that the upwelling tube could be compressed for the convenience of transportation(see fig.2(b)).

C. Performance of two different tubes

The configuration of the upwelling tube observed by the underwater remote operated vehicle (ROV) during the Qiandao lake test was shown in Fig.3, wherein the first test was shown in Fig.3(a), which was conducted with the PVC ventilation pipe in September 2011, as could be seen, the shape of the upwelling tube was maintained well underwater. While in Fig.3 (b), the lake test with the second structure of upwelling pipe conducted in December 2012, where we could find that the upwelling tube underwater suffered more serious deformation, common with shrinkage occurring between the connected supporting rings, especially for that with diameter of 0.5m, the deformation was proved particularly serious.

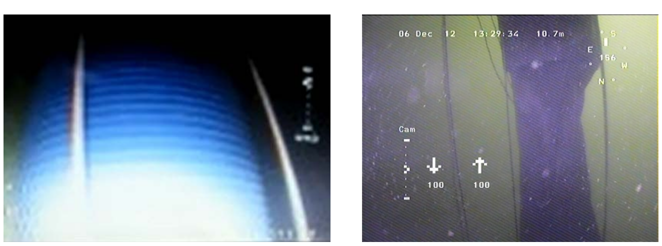

Fig. 3. Shapes of the upwelling tubes when working underwater of the two lake tests: (a) underwater shape of the upwelling tube during the first test; (b) underwater shape of the upwelling tube during the second test

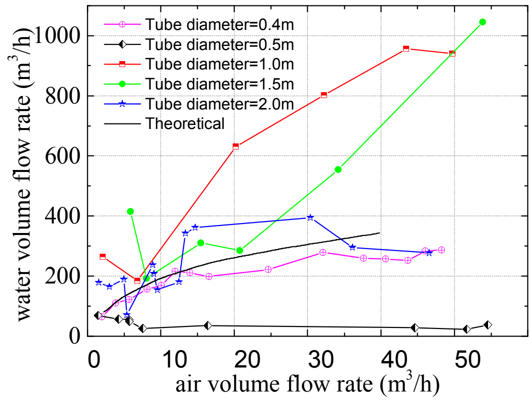

Fig. 4. Variations of water volume flow rate vs. air volume flow rate for tubes with different diameters

For the first and the second lake tests, the variation relationships between the airflow rate and the flow rate of the upwelling water were shown in Fig.4, as could be seen, for the first one employing upwelling tube with diameter of 0.4m, as the airflow increased, the upwelling flow stably grew; while for the second, the underwater shrinkage of the 0.5m-diameter upwelling tube brought about rather small upwelling flow, moreover, with the increasing airflow, the upwelling flow got smaller, and the tube shrinkage could be distinguished to be more obvious. While for the 2m-diameter upwelling tube, the curve suffered very severe fluctuation and exhibited unstable, we could find through analysis that since the power of the air pump was fixed, the underwater gas-injecting pressure was constant, then the maximum airflow was constant, as a result, the air flow could not generate sufficient bubble flow over full range of the diameter (with the nozzle shape fixed), thereby water above the nozzle flew with local reversing flow. Considering the difficulties in sea trial and transportation, the structure of the upwelling tube needed to be optimized, concretely, to increase the quantity of the support rings at the shrinkage-prone section and to reduce the distance between the support rings could enable the upwelling tube with inner support rings to be possessed with the same performance with that of the PVC ventilation pipe, wherein the theoretical value curve was established based on the 0.4m-diameter upwelling tube, from which we could obtain that the variation trend of the theoretical values proved consistent with the measured values of the 0.4m-diameter upwelling tube, and also numerically closer to each other.

III. WAVE POWERED AIR BOOSTER

A. Design and components

The air booster pump captured the ocean wave energy through the floater, and then continued with air collection and compression. The whole wave-powered air-lift upwelling system working in the sea was shown in Fig.5, and the main structure of the air booster pump in Fig.6.

The upwelling system could be divided into the floating device part and the fixed device one, wherein the former mainly included the buoy, support, guide rail and the upper seal cover, while the latter principally consisted of for double-acting air pneumatic cylinders, the supporting frame, slide rail and the driving chain. Moreover, the fixed device was anchored to the seafloor, while the buoy fluctuated with the waves, and the relative transmission generated was finally converted to the rotation of the drive shaft by the joint action of the rack and the gear to drive the crank to rotate, when the link lever connected to the crank, i.e. the double-acting pneumatic cylinder would achieve its extension and retraction, that was how the air collection and compression realized.

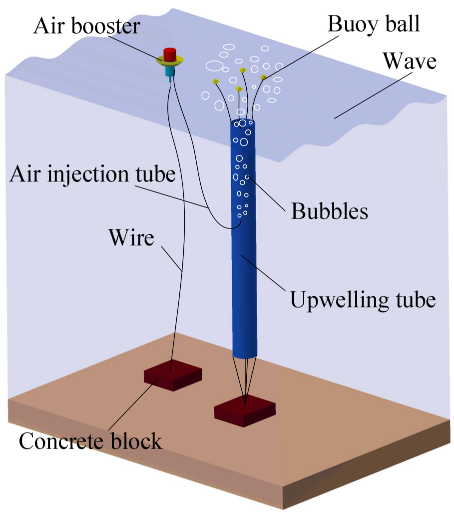

Fig. 5. Working diagram of the artificial wave-powered air-lift upwelling

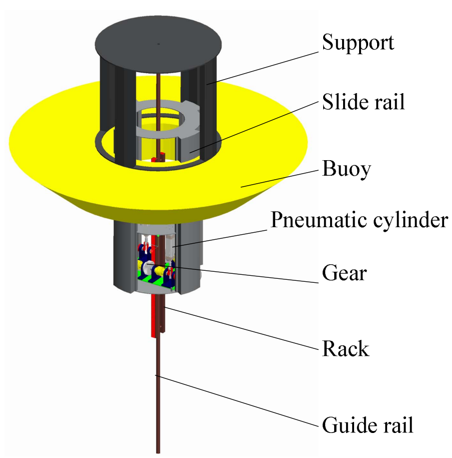

Fig. 6. Diagrammatic sketch of the air booster pump

Rhinefrank, etc. had ever conducted a linear test bed (LTB) experiment to test the efficiency of the PTO device[16], wherein the linearly-moving device was employed to drag the PTO (power take-off) device, and the characteristics of rated power, efficiency, force and speed were focused to be tested through several groups of loading tests. Before the implementation of the sea trial in this project, it is indispensable to conduct the principle test on the prototype in the lab, so as to optimize the design of the prototype structure. In this paper, the hydraulic platform was employed to drag the prototype of the air booster pump to validate its performance, wherein the reciprocating push-and-pull motion of the hydraulic platform was used to simulate the wave fluctuation. The prototype of the air booster pump for the laboratory test was based on the air booster pump with the removal of the floater and the guiding rail, etc., which was directly connected with the hydraulic cylinder simulating the up-and-down wave movement. Furthermore, the sealing situation was also simplified, with the final model shown in Fig.7.

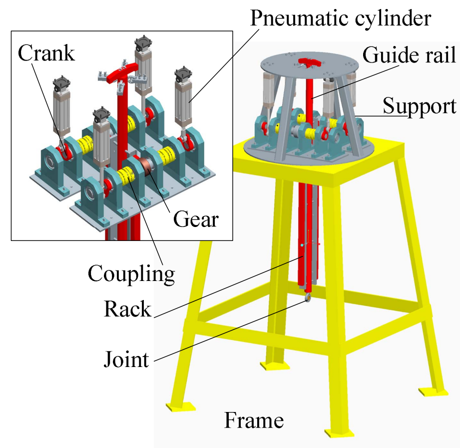

Fig. 7. 3-dimensional model of the wave-powered air booster pump prototype

B. Numerical simulation model

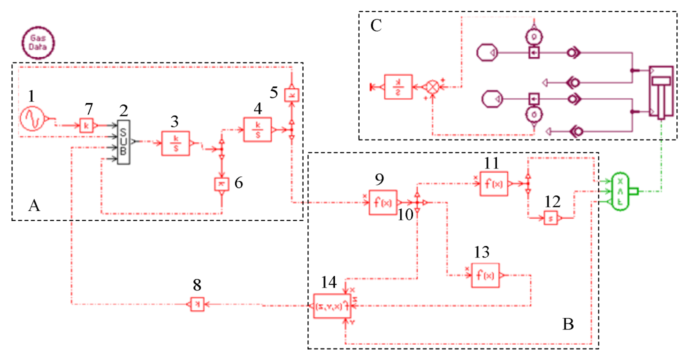

Fig. 8. AMESim model of the air booster pump

For the buoy, the following mechanical equation could be established：

$$(m_m + m_r(\omega))\frac{d^2z}{dt^2} + (R_v + R_f + R_r(\omega))\frac{dz}{dt} + F_f + F_{pto} = F_e \qquad (3)$$

Wherein R_v denoted the viscous damp coefficient of the seawater, R_f the frictional coefficient of the mechanical drive, R_r the dissipative damp coefficient, F_f the composite force of the buoyancy, the gravity and the anchoring force, here we called it net buoyancy, F_{pto} the reacting force exerted on the buoy by the PTO structure, ω the circular frequency, m_m the mass of the buoy itself, and m_r the added mass generated by the rising-up of water surrounding the buoy.

In this paper, the simulation software-Amesim would be employed to conduct numerical computation on the performance of the air booster pump. In the model, Box A denoted the interaction between the buoy and the waves. And Mark 1 denoted the wave oscillation, here, we would only investigate the influence of regular waves (no mutual superposition between them) whose displacement exhibited sinusoidal variation with the velocity. And what Mark 7 denoted was called the excitation acceleration coefficient, i.e. the transformation coefficient between the exciting force and the amplitude, which represented that the exciting force that the buoy suffered was proportional to the wave displacement. Moreover, Mark 2 showed the stress condition of the buoy which could be conveniently obtained according to Eq.3, Mark 3 its velocity, and Mark 4 its translational speed. Additionally, the parameter shown by Mark 5 was the defined net buoyancy acceleration coefficient, with the calculation equation

$$\kappa_f = F_f / (m_m + m_r) \tag{4}$$

And that by Mark 6 denoted the defined dissipative acceleration coefficient, computed by

$$\kappa_r = R_r / (m_m + m_r) \tag{5}$$

Box B represented the crank and link lever mechanism of the air booster pump prototype, whose input was the buoy displacement, and outputs were the velocity and displacement of the end connected to the piston rod of the piston-type air pump, with feedback of the acting force to the buoy. Therein, what Mark 9 showed was converting the buoy position to the rotation angle of the crank; Mark 11 got the angle variation converted to the length variation of the air pump on the link lever; Mark 12 finally obtained the velocity by differentiating the displacement; Mark 13 was the included angle between the air cylinder and the platform plane; Mark 14 calculated the force acting on the rack based on torque equilibrium.

In Box C, the gas-injecting process by the gas-collection device to the deep-sea position with a fixed pressure was simulated to be that to an air reservoir with infinitely large volume, and finally, the flow rate was integrated to output the flow.

Let a spherical 0.5m-radius buoy be under waves with height of 0.5m and period of 5.3s (the following simulation experiments was conducted in this wave state), and the following parameters for simulation were eventually obtained as per the calculation method above.

According to the dimensions of the crank and link lever mechanism in the designed structure, the feedback coefficient from the PTO device to the buoy was eventually set (as shown by Mark 8 in Fig.8). With the feedback force added, the variation of the buoy displacement with the incident wave was shown in Fig.9.

Only when the wave reached a certain height could the buoy overcame the feedback force of the PTO device and rose. On the other hand, after the wave fell, as the buoyancy of the buoy gradually decreased, the buoy would overcome the feedback force of the PTO device under the gravity and eventually made a downward displacement. And such experimental results could also satisfy the qualitative analysis of the whole process; as a consequence, it was obviously visible that the 0.5m-radius buoy could already enable the device to obtain a free frequency similar to the circular frequency of the wave, which will result into resonance between the wave and the buoy.

TABLE I. PARAMETER TABLE FOR FLOATER WITH RADIUS OF 0.5M

Name	Symbol	Value
Peorid	T	5.3
Wave height	A	0.5
Gravity acceleration	g	9.8
Spherical buoy radius	a	0.5
Seawater density	ρ	1000
mass of the isopyknic water with the buoy	m_m	261.8
Additional mass	m_r	228.0069
Total mass	m	489.8069
Exciting acceleration coefficient	κ_e	14.30876
Dissipative acceleration coefficient	κ_r	0.085416
Net buoyancy acceleration coefficient	κ_f	15.71419
wave circular frequency	ω	1.185509
Wave number	k	0.143411
Additional mass coefficient	μ	0.87092
Dissipative damp coefficient (dimensionless)	ϵ	0.1348
Dissipative damp coefficient	R_r	41.83739
Net buoyancy coefficient		7696.92
Exciting force coefficient		7008.529
buoy volume		0.5236
Area of buoy at waterline	S_b	0.7854
Reaction acceleration coefficient	κ_{ca}	0.0205

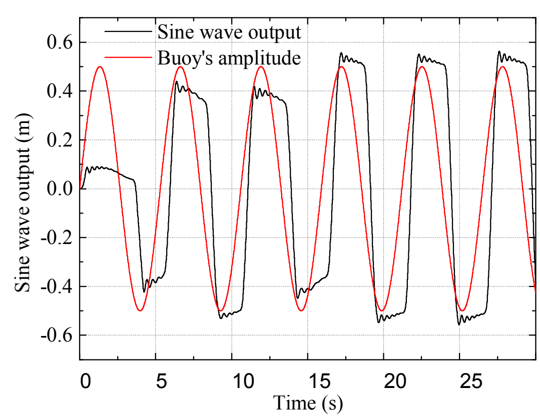

Fig. 9. Displacement variation of the 0.5m-radius buoy with the incident wave (under load)

Fig.10 shows that the air volume output enduring 4 Bar pressure accumulates with the time, which indicates that the air flow rate output maintains unchanged and benefits to stabilize the air-water mixed flow upwelling in the upwelling tube.

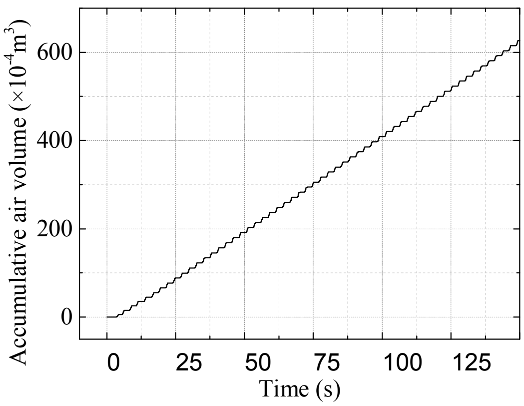

Fig. 10. the accumulative air volume output vs. time

IV. CONCLUSIONS

(1) The energy equilibrium equation of the air-lift upwelling was established, which could favorably predict the upwelling water amount of the lower layer by means of different upwelling tubes.

(2) Through two lake tests over the air-lift upwelling, it was found that for upwelling tube with inner support rings, the arrangement of the support rings inside needed to be optimized, so as to reduce the inward shrinkage of the upwelling tube resulted from the up-flowing of the gas-water mixture.

(3) The air booster pump prototype simulating the wave-powered gas collection and compression was eventually designed, whose natural frequency, through computation by the simulation software, proved similar to the circular frequency of the wave, when the conversion efficiency of the wave energy achieved the maximum.

ACKNOWLEDGMENT

The authors would like to thank the crews of Qiandao Lake test barge for their essential support.

REFERENCES

[1] Scott, Stuart A.;Davey, Matthew P.;Dennis, John S.;Horst, Irmtraud;Howe, Christopher J.;Lea-Smith, David J.;Smith, Alison G. Biodiesel from algae: challenges and prospects. Current Opinion in Biotechnology. 2010, 21, 3, 277-286.

[2] Villasante, Sebastián;do Carme García-Negro, María;González-Laxe, Fernando;Rodríguez, Gonzalo Rodríguez. Overfishing and the Common Fisheries Policy: (un)successful results from TAC regulation? Fish and Fisheries. 2011, 12, 1, 34-50.

[3] Kirke, Brian. Enhancing fish stocks with wave-powered artificial upwelling. Ocean & Coastal Management. 2003, 46, 9–10, 901-915.

[4] Scott, Stuart A.;Davey, Matthew P.;Dennis, John S.;Horst, Irmtraud;Howe, Christopher J.;Lea-Smith, David J.;Smith, Alison G. Biodiesel from algae: challenges and prospects. Current Opinion in Biotechnology. 2010, 21, 3, 277-286.

[5] Ouchi, K.;Murphy, A. J., Real sea experiment of ocean nutrient enhancer "TAKUMI" upwelling deep ocean water, in Proceedings OCEANS 2003. Proceedings22-26 Sept. 2003 2003, Volume 2, p. 881 Vol.2.

[6] Liu, Clark C. K.;Jin, Qiao. Artificial upwelling in regular and random waves. Ocean Engineering. 1995, 22, 4, 337-350.

[7] Liu, C. Research on artificial upwelling and mixing at the University of Hawaii at Manoa. IOA Newsletter. 1999, 10, 4, 1-8.

[8] White, Angelicque;Björkman, Karin;Grabowski, Eric;Letelier, Ricardo;Poulos, Steve;Watkins, Blake;Karl, David. An open ocean trial of controlled upwelling using wave pump technology. Journal of Atmospheric and Oceanic Technology. 2010, 27, 2, 385-396.

[9] Kithil, Philip W. "Oceanic Layers Modification Methods, Apparatus, Systems and Applications." U.S. Patent Application 12/056,480, filed March 27, 2008.

[10] Linden, PF, On the structure of salt fingers, in Proceedings Deep Sea Research and Oceanographic Abstracts1973, Volume 20, Elsevier, p. 325-340.

[11] Lovelock, James E;Rapley, Chris G. Ocean pipes could help the Earth to cure itself. Nature. 2007, 449, 7161, 403-403.

[12] Tsubaki, Koutaro;Maruyama, Shigenao;Komiya, Atsuki;Mitsugashira, Hiroaki. Continuous measurement of an artificial upwelling of deep sea water induced by the perpetual salt fountain. Deep Sea Research Part I: Oceanographic Research Papers. 2007, 54, 1, 75-84.

[13] Liang, Nai-Kuang;Peng, Hai-Kuen. A study of air-lift artificial upwelling. Ocean Engineering. 2005, 32, 5–6, 731-745.

[14] Peng, Hai-kuen, 1999, Experimental and Theoretical Study of Air-lift Artificial Upwelling [Ph.D: National Taiwan University.

[15] McClimans, T. A.;Handå, A.;Fredheim, A.;Lien, E.;Reitan, K. I. Controlled artificial upwelling in a fjord to stimulate non-toxic algae. Aquacultural Engineering. 2010, 42, 3, 140-147.

[16] Fan, Wei;Chen, Jiawang;Pan, Yiwen;Huang, Haocai;Arthur Chen, Chen-Tung;Chen, Ying. Experimental study on the performance of an air-lift pump for artificial upwelling. Ocean Engineering. 2013, 59, 0, 47-57.

[17] Rhinefrank, K.;Schacher, A.;Prudell, J.;Brekken, T. K. A.;Stillinger, C.;Yen, J. Z.;Ernst, S. G.;Von Jouanne, A.;Amon, E.;Paasch, R.;Brown, A.;Yokochi, A. Comparison of Direct-Drive Power Takeoff Systems for Ocean Wave Energy Applications. Oceanic Engineering, IEEE Journal of. 2012, 37, 1, 35-44.